373. Massarsch, K.R, Fellenius, B.H. 2017. Evaluation of resonance compaction of sand fill based on cone penetration tests. Ground Improvement. Proceedings of the Institution of Civil Engineers. Paper 1700004, ICE Publishing, pp. 1 - 10.

Ground Improvement

Evaluation of resonance compaction of sand fills based on cone penetration tests
Massarsch and Fellenius

ice | proceedings

Proceedings of the Institution of Civil Engineers

http://dx.doi.org/10.1680/jgrim.17.00004
Paper 1700004
Received 11/01/2017 Accepted 16/05/2017
Keywords: land reclamation/landfills/site investigation

ice Institution of Civil Engineers
publishing

Evaluation of resonance compaction of sand fills based on cone penetration tests

1 Karl Rainer Massarsch Dr. Tech. Eur. Ing.
Consulting Engineer, Geo Risk & Vibration Scandinavia AB, Stockholm, Sweden (corresponding author: rainer.massarsch@georisk.se)
(Orcid:0000-0001-8906-7452)

2 Bengt H. Fellenius Dr. Tech.
Consulting Engineer, Sidney, BC, Canada


A case history in which a 14 m thick sand fill was compacted by the resonance compaction method is presented. The execution of the resonance compaction method (equipment and process) is described in detail. In this method, a heavy vibrator is mounted on top of a purpose-built compaction probe that has large openings in the wall to minimise its mass, as low mass enhances compaction. The vibration amplification effect, which occurs when the vibrator–probe–soil system is operated at system frequency, results in an enhanced compaction effect and reduced compaction time. The results of field trials where the compaction effect was measured in terms of ground settlement (compression) and cone penetration tests (CPTs) are reported. The increase in cone stress and sleeve friction was measured 2 d and 7 d following compaction. An important aspect of deep vibratory compaction is a permanent increase in the horizontal effective stress, which is reflected by the change in sleeve friction after compaction. Based on CPT results, it is possible to determine the modulus number and preconsolidation stress, which is needed for settlement analyses according to the tangent modulus method.

Notation

a	empirical modulus modifier
C_M	cone stress adjustment factor
f_s	sleeve friction
K_0	coefficient of earth stress at rest for normally consolidated sand
K_1	coefficient of earth stress at rest for compacted sand
K_A	coefficient of lateral effective stress after compaction
K_B	coefficient of lateral earth stress at rest before compaction
K_D	dilatometer horizontal stress index
m	modulus number
q_c	cone stress
q_{cM}	adjusted cone stress
R_f	friction ratio ($f_s/q_c \times 100$)
β	empirically determined exponent
σ'_m	mean effective stress
σ_r	reference stress = 100 kPa
σ'_v	vertical effective stress
ϕ'	effective friction angle

1. Introduction

In spite of the growing number of land reclamation projects built up from sand fills in need of compaction, little practical guidance can be found in the geotechnical literature regarding the planning, design, execution and monitoring of sand fill compaction. The density of sand placed under water (subaqueous fill) is generally lower than that placed above groundwater (subaerial fill). Lee (2001) found that the placement technique is the single most important factor controlling the geotechnical behaviour of a given type of sand when placed as a hydraulic fill. The weakest zone is generally located just beneath the water level. The range of densities achievable by the hydraulic placement of sand is typically at the boundary between the values giving acceptable performance and those resulting in unacceptable performance. Therefore, it is, at an early stage of a project, important to assess whether compaction is needed and, if so, to what degree. In most cases, compaction of a sand fill is required to reduce the total and differential settlements. In addition, the effect of cyclic loading due to seismic or other dynamic forces (wave loading, blasting, heavy traffic) may need to be considered. This paper focuses on the performance of uncompacted and compacted sand fills during static loading. However, several of the conclusions also apply to cyclic and seismic loading of compacted sand fills.

Sand fills without compaction can be assumed to be normally consolidated. This important – but not generally appreciated – aspect offers the opportunity to assess more accurately the in situ stress conditions prior to and after compaction, including determining the degree of required compaction.

Massarsch and Fellenius (2014) outlined a concept particularly developed for the design of sand fill projects, which is more rigorous than general design procedures. This paper describes how the design concept can be applied in practice. A variety of sand compaction methods can be used to meet the design requirements. One method, which has found increasing application, is resonance compaction (Massarsch, 1991a, 1991b). The principles of application of resonance compaction in engineering practice have been described by Massarsch and Fellenius (2005). This paper presents a case history of resonance compaction applied to a major land reclamation project in Hong Kong.

2. Resonance compaction method

The resonance compaction method was developed in the early 1980s, using different types of compaction probes. The first practical application of changing the vibrator operating frequency was described by Massarsch and Broms (1983). The compaction probe consisted of a steel rod with laterally extending blades (called a 'VibroWing'). Later, a three-bladed compaction probe was used for liquefaction mitigation, as described by Neely and Leroy (1991) and Van Impe *et al.* (1994). The next step in the development of the system was the use of a flexible compaction probe in which the weight of the compaction probe was reduced and the interaction between the probe and the soil was increased (Massarsch, 1991a, 1991b). One form of resonance compaction was applied to improve the sand fill at the reclamation in Changi East, Singapore, involving the formation of 2000 ha of land (Choa *et al.*, 2001). For the same project, Krogh and Lindgren (1997) performed extensive investigations, such as vibration measurements at and below the ground surface during the compaction work. The significance of the vibrator operating frequency on the compaction process was studied in great detail. They showed that vertically oscillating probes generated high horizontal stresses in the ground. The compaction effect of different methods at the Changi sites was compared by Bo *et al.* (2014). Vibratory compaction using vertically oscillating probes can be a technically and economically competitive ground improvement method. However, it requires the use of appropriate equipment and that the compaction process is carried out by competent personnel. The objective of this paper is to provide useful guidelines for the efficient planning and execution of resonance compaction projects.

2.1 Compaction process

The resonance compaction method uses the vibration amplification effect that is created when the operating frequency of the vibrator is adjusted to the resonance frequency of the vibrator–probe–soil system (Massarsch, 1991b). A powerful hydraulic vibrator with variable operating frequency is mounted on top of a purpose-built compaction probe. The longitudinal section and cross-section of the probe, which has a double-Y shape, are shown in Figure 1. An important aspect is that the weight of the probe is significantly reduced by the incorporation of circular openings in the probe walls. The probe is guided by a lead to ensure vertical penetration. The openings increase the interaction between the oscillating probe and the surrounding soil and, thus, the efficiency of the vibration emissions from the compaction probe.

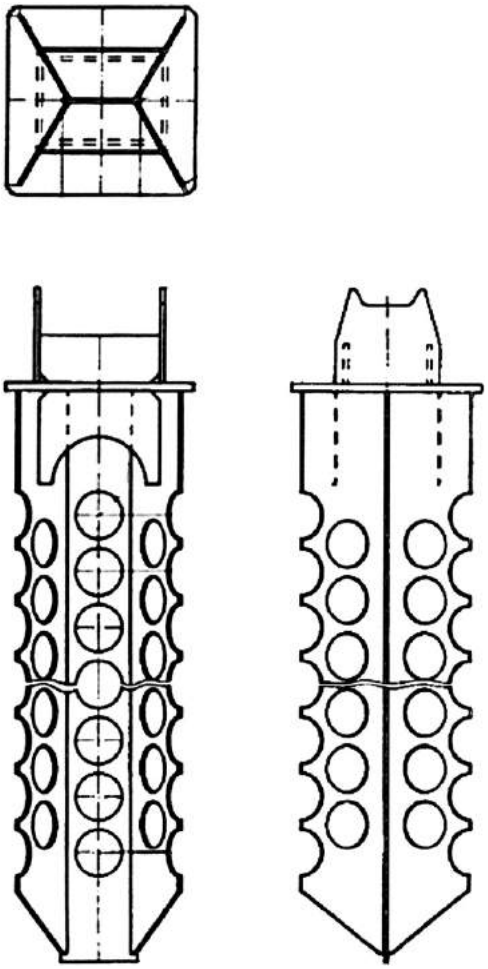

Figure 1. Longitudinal profile and cross-section of resonance compaction probe

2.2 Frequency control

When using the resonance compaction unit, geophones measuring vibration velocity are installed on the ground surface, typically at a distance of 4 m from the compaction point. The vibration measurements are fed into a data acquisition system together with other compaction parameters such as probe penetration depth, vibrator acceleration, operating frequency and the hydraulic pressure of the vibratory system (powerpack). The system principles have been described in detail by Massarsch and Fellenius (2005). Figure 2(a) shows a geophone adjacent to a flexible compaction probe and Figure 2(b) shows the computer-controlled display used for the control of probe movement and vibrator frequency.

(a) (b)

Figure 2. Monitoring of resonance compaction, controlling probe movement and frequency variation: (a) geophone for control of vibrator frequency; (b) control panel for resonance compaction

A fundamental aspect of resonance compaction is the variation of vibrator frequency. In granular soil, when the probe is operated at a high frequency (approximately >35 Hz), substantially higher than the resonance frequency of the vibrator–probe–soil system, surface friction along the compaction probe is effectively reduced and the main resistance originates at the toe of the compaction probe. Thus, in loose granular soil, the probe sinks into the ground at high penetration speed and the ground vibrations are low. Most of the vibration energy is dissipated as heat along the probe surface. The penetration speed of the probe (when excited at high frequency) reflects the soil resistance at the toe of the probe. When the probe penetrates freely and is not held back, the probe penetration speed can then be related to the cone stress measured by the cone penetration test (CPT). Or, the CPT sounding (cone stress, q_c) can be used on a site-specific basis in estimating the efficiency of the compaction effort in terms of probe penetration speed.

When the vibrator frequency is gradually reduced, two distinct phenomena can be observed: the probe penetration speed slows down and the intensity of the ground vibration increases (Massarsch and Fellenius, 2005). When the operating frequency of the vibrator approaches the resonance frequency of the vibrator–probe–soil system, the probe penetration can stop completely; at the same time, ground vibrations reach a maximum. At this stage, the vibrator energy is efficiently transmitted to the soil along the probe surface and vibration compaction is most effective.

In loose to medium dense, water-saturated granular soil, resonance can cause liquefaction. The probe then oscillates in the liquefied soil (acting as a heavy liquid) and no ground vibrations are transmitted to the soil as little or no friction exists along the probe. As the vibration continues, the excess pore water pressure dissipates, effective stress builds up and the friction between the probe surface and the surrounding soil again increases along the probe. The end result is a reduction of the soil volume (compaction), an increase in soil density (modulus) and a permanent preconsolidation effect, as described by Massarsch and Fellenius (2014).

2.3 Horizontal stress increase

An important – but often neglected – effect of vibratory compaction is the creation of high horizontal stresses, which are caused by the friction between the probe surface and the surrounding soil. Vibration measurements at the ground surface and several metres below show that the vertically oscillating probe induces high horizontal stresses (Krogh and Lindgren, 1997; Massarsch, 2002). As a result of the strong, horizontal stress pulses caused by the vertically oscillating probe, permanent increases of horizontal stresses are created in the ground. These have been measured on a large number of compaction projects and show an increase in CPT sleeve friction, f_s, and the dilatometer horizontal stress index, K_D (Balachowsky and Kurek, 2016; Brown, 1989; Gallon and Netterman, 1996; Jendeby, 1992; Massarsch, 1994; Massarsch and Fellenius, 2005; Van Impe *et al.*, 1994). The permanent increase in horizontal effective stress causes a preconsolidation effect that is reflected by a rise in the overconsolidation ratio (OCR).

3. Resonance compaction – a case history

The case history describes the compaction of a hydraulic fill at Yam O, Hong Kong, which was part of the North Lantau

expressway and the airport express line. The project site is located ~11 km from the new Hong Kong airport at Chep Lap Kop. A part of the area had to be reclaimed and dredged. 'Fresh water sand' was placed by bottom dumping and sand spraying. The thickness of the sand fill varied between 10 and 18 m. The fill included calcareous material (shells) and occasional zones or pockets of silt and clay. The hydraulically placed sand fill rested on a layer of stiff clay and needed compaction to meet the design criteria. The groundwater level fluctuated with the tide, but was, on average, located about 2 m below the final surface of the fill, as designed. In order to meet the stringent settlement requirements, the hydraulic fill had to be compacted. The contractor chose the resonance compaction method.

3.1 Geotechnical conditions

The geotechnical design was based on the results of CPTs. According to the project specifications, a minimum 10 MPa after-compaction cone stress was required throughout the sand fill. A large number of CPTs was carried out on site. One aspect was to evaluate the potential increase in cone stress with time after compaction. Therefore, CPTs were also performed in a trial area at different time periods (2 d and 7 d after compaction). The project was described in detail by Gallon and Netterman (1996).

Before the start of production work, trial compaction was carried out in a representative area to establish the optimal compaction procedure (i.e. spacing between compaction points and duration of compaction). The compaction effect was monitored by settlement measurements and comparison of CPT results prior to and after compaction. Three CPTs were performed prior to compaction. Cone stress, q_c, and sleeve friction, f_s, were measured. In order to facilitate comparison of test results prior to and after compaction, the CPT data were filtered using geometric mean over depth intervals of ±50 mm. In a sand fill, the pore water pressure has only a slight effect on the measured cone stress and, therefore, the uncorrected q_c value is used in this paper. The average cone stress, q_c, and sleeve friction, f_s, measured before compaction are shown in Figures 3(a) and 3(b), respectively. Down to 5·5 m depth, the cone stress was lower than 5 MPa and increased thereafter to between 5 and 7·5 MPa. The sleeve friction was almost constant (10 kPa) down to a 5·5 m depth and increased below this depth to between 15 and 30 kPa.

3.2 Compaction process

Resonance compaction was carried out with a Müller MS 100HF variable frequency vibrator with an MS-A560 power pack. The vibrator weighed 109 kN and was supported by a 100 t crawler crane. The machine used for resonance compaction is shown in Figure 4. The vibrator could generate a maximum centrifugal force of 2500 kN and a maximum eccentric moment of 100 kg (1000 J). The maximum pulling power of the vibrator was 600 kN. The vibrator frequency could be varied gradually at full power from 5 to 36 Hz. The maximum vibration amplitude of the vibrator without probe was 26 mm (double amplitude).

Prior to the start of the production phase, trial compaction was carried out. During the first compaction pass, the compaction grid spacing was 4·2 m × 3·6 m. During the second pass, the intermediate points at the centre of the initial grid were compacted. The distance between compaction points

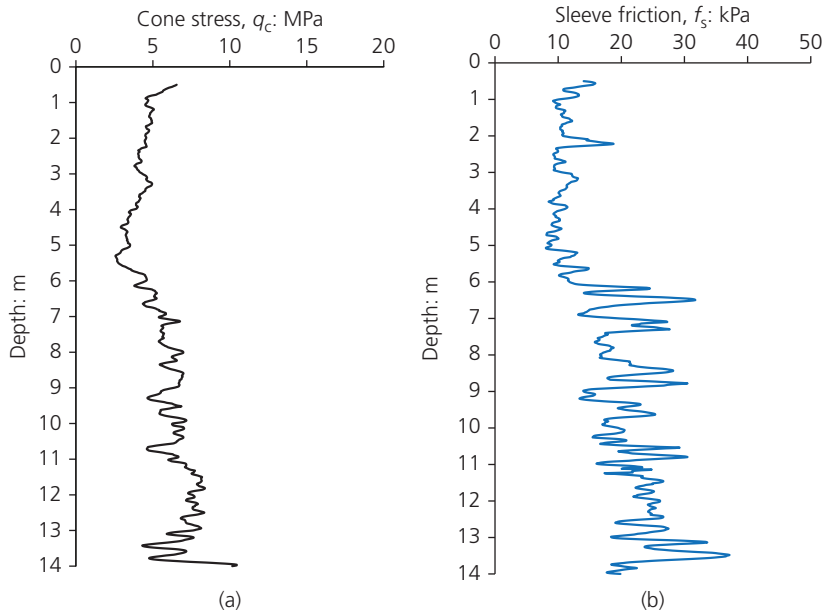

Figure 3. Average of three CPTs in trial area before compaction. The results are shown as geometric mean over depth intervals of ±50 mm: (a) cone stress and (b) sleeve friction

(a) (b)

Figure 4. Resonance compaction equipment used at Yam O site. Note the collection of ground water around the probe during compaction: (a) resonance compaction machine; (b) compaction probe with circular openings

after completion of the second pass was 2·8 m. At seven of the points, the duration of compaction was 5 min and at the remaining six points the duration was 10 min (Figure 5).

3.3 Settlement measurements

Within the trial area, the groundwater table was about 2 m below the ground surface. The thickness of the sand fill was ~14 m. During compaction, a large crater with a diameter corresponding to approximately twice the diameter of the compaction probe formed. In addition, a large settlement cone, extending up to 10 m from the compaction crater, could be observed. At each compaction point, the duration of effective compaction was 5 and 10 min, respectively. During the initial phase of vibratory compaction, the sand fill liquefied and the groundwater level rose to the surface in the compaction point (Figure 4(b)). It is interesting to note that liquefaction did not occur when compaction was carried out during the second compaction pass; the soil was sufficiently densified to prevent liquefaction. Thus, monitoring of resonance compaction could potentially be used as a full-scale testing device with respect to liquefaction.

Before compaction, the surface within the trial area had been levelled. The day after the first round of compaction, the surface was again levelled without an addition of sand fill, and its elevation was surveyed. The difference in the before-compaction elevation gave the average settlement of the surface due to the compaction effort. The results of settlements and relative compression within the compaction depths are compiled in Table 1.

Average settlement within the trial area was 0·64 m and the average compression was 4·4%. During the second compaction pass, settlements were generally lower than during the first pass.

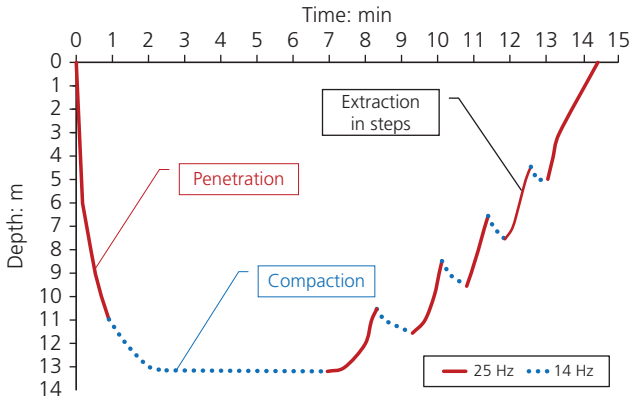

Figure 5. Execution of resonance compaction process. Probe penetration to 11 m at high frequency (25 Hz); resonance compaction from 11 to 13 m at resonance frequency (14 Hz). Extraction in steps at high frequency (25 Hz) and re-penetration at low frequency. Probe extraction from 5 m depth at high frequency.

No clear indication could be found that an increase in the duration of compaction would result in a significantly higher soil layer compression and, thus, improved compaction. It was thus decided to adopt a compaction phase of 5 min, resulting in a total duration of compaction of ~15 min at each compaction point.

4. Evaluation of compaction effect

4.1 CPT results

In order to evaluate the effect of time on the compaction effect, CPT measurements were performed 2 d and 7 d after compaction. An attempt was made to perform CPT measurements in between the compaction points (largest distance from

Table 1. Settlement and compression of compacted layer

Duration of compaction: min	Settlement: m	Compaction depth: m	Compression: %
5	0·60	14·4	4·17
5	0·65	14·2	4·58
5	0·76	14·0	5·43
5	0·64	14·5	4·41
5	0·57	14·4	3·96
5	0·62	14·5	4·28
10	0·62	14·5	4·28
10	0·53	14·6	3·63
10	0·77	14·3	5·38
10	0·60	14·0	4·29

compaction point). Due to the post-compaction surface levelling, however, it was difficult to locate the exact spot. The measured cone stress and sleeve friction are shown in Figure 6. The average cone stress exceeded the minimum value of 10 MPa. Both the cone stress and the sleeve friction increased significantly. No clear time effect (2 d and 7 d) could be observed, but the increase in cone stress and sleeve friction was higher after 7 d in the top 5 m of the fill. However, the difference in compaction effect is most likely related to the variability of the sand fill, which contained layers of silt and calcareous material. It can be expected that, with time, there will be an equalisation of the horizontal effective stress.

The cone stress increased due to compaction, as shown in Figure 7(a). The increase was larger in the upper, about 5 m, part of the compacted sand (by 2–3 times) and less pronounced below that depth (by 1·5–2 times). Figure 7(b) shows that the sleeve friction also increased. In contrast to the cone stress increase, the increase in sleeve friction was almost constant throughout the fill, an aspect that is rarely appreciated. The increase in sleeve friction was between 1·5 and 4 times the sleeve friction in the uncompacted fill, with an average value of 2·5. As is shown below, this effect can be of great practical significance.

Massarsch and Fellenius (2014) pointed out that the cone stress is affected by the mean effective stress. In order to compare cone stress values, it is necessary to eliminate the effect of depth. This proposed procedure transforms the measured cone stress, q_c, at a given depth to a cone stress, q_{cM}, at a mean effective stress of 100 kPa. By applying a cone stress adjustment factor, C_M, it is possible to calculate the stress-adjusted cone stress

$$1. \quad q_{cM} = q_c C_M = q_c \left(\frac{\sigma_r}{\sigma'_m}\right)^{0.5}$$

where σ_r is the reference stress = 100 kPa and σ'_m is the mean effective stress. At normally consolidated conditions (prior to compaction), the coefficient of horizontal effective stress, K_0, can be estimated from the relationship proposed by Jáky (1948)

$$2. \quad K_0 \sim 1 - \sin(\phi')$$

where ϕ' is the effective friction angle. In compacted fills, the horizontal stress increases.

This increase in horizontal effective stress can be estimated from the ratio between sleeve friction after compaction and the

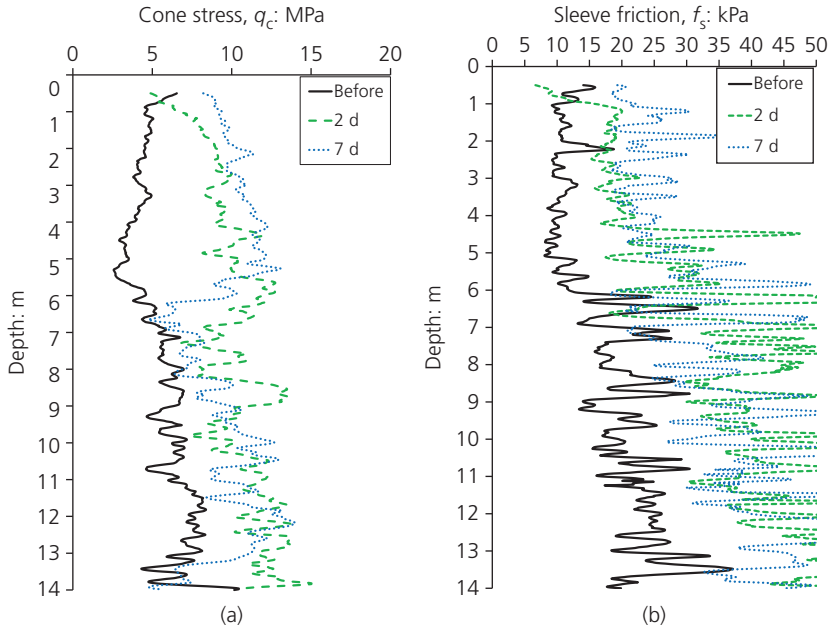

Figure 6. Average of three CPTs in trial area prior to and 2 d and 7 d after compaction: (a) cone stress; (b) sleeve friction

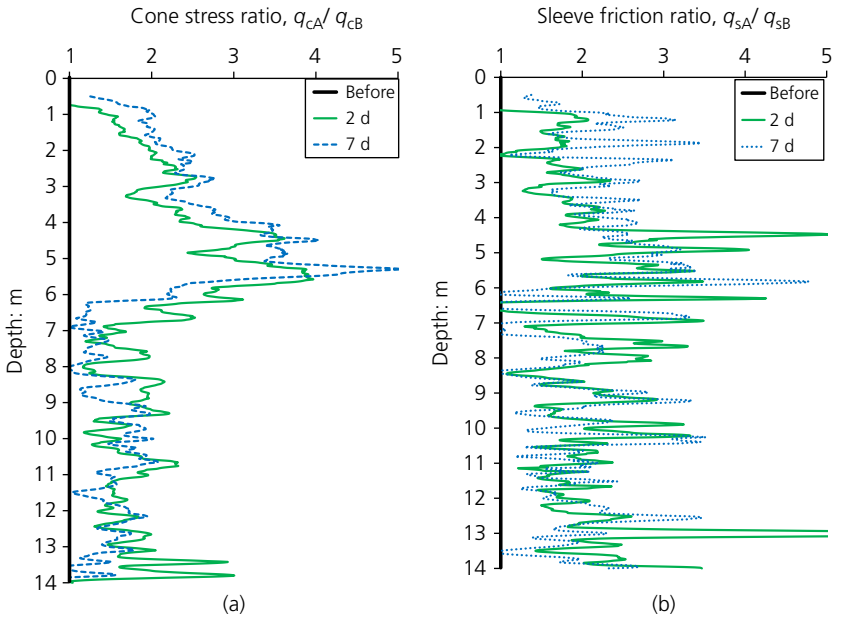

Figure 7. Increase in cone stress and sleeve friction prior to (B) and 2 d and 7 d after (A) compaction: (a) increase in cone stress; (b) increase in sleeve friction

value prior to compaction. The ratio of the horizontal effective earth stress after and before compaction can then be approximated from the relationship

$$3. \quad \frac{K_A\,\sigma'_A}{K_B\,\sigma'_B} \simeq \frac{f_{sA}}{f_{sB}} \frac{\tan(\phi'_B)}{\tan(\phi'_A)}$$

where the subscripts A and B indicate the state before and after compaction, respectively. The coefficient of horizontal earth stress after compaction, K_A, can now be estimated from

$$4. \quad K_A = \frac{f_{sA}}{f_{sB}} K_B \frac{\tan(\phi'_B)}{\tan(\phi'_A)}$$

The vertical effective stress will remain practically unchanged, but, as the density increases due to compaction, the friction angle will increase. The ratio of tangents becomes 1·04 with a post-compaction friction angle of 34° and increases ~0·04 with each degree of increase in friction angle. However, for practical purposes, the effective friction angle, ϕ', and the effective vertical stress, σ'_v, can be taken as remaining essentially unchanged following compaction. The coefficient of horizontal earth stress at rest prior to compaction, K_B, can be estimated from Equation 2. If the friction angle of the uncompacted sand fill is assumed to be $\phi' = 33°$, according to Equation 2, $K_B = 0{\cdot}46$.

Figure 7(b) shows the sleeve friction, f_{sA}/f_{sB}, due to compaction, with an average increase of about 2. Thus, the increase in horizontal stress can be used to calculate the coefficient of horizontal earth stress after compaction, $K_A = 0{\cdot}92$. Note that K_A is not the active earth pressure coefficient. The mean effective stress, σ'_m, needed in Equation 1 can be determined according to

$$5. \quad \sigma'_m = \sigma'_v \left(\frac{1 + 2K_A}{3}\right)$$

where σ'_m is the mean effective stress, σ'_v is the vertical effective stress and K_A is the coefficient of horizontal stress after compaction.

It is now possible to determine the adjusted cone stress, q_{cM}, according to Equation 1. In Figure 8(a), the adjusted cone stress is shown prior to compaction, as well as 2 d and 7 d after compaction. It can be concluded that, as a result of stress adjustment, the cone stress increases close to the ground surface, due to the decreasing mean effective stress.

Another important aspect of compaction is the preconsolidation effect. Relationships between the increase in horizontal effective stress and the OCR have been proposed in the geotechnical literature, and have been summarised by Massarsch and Fellenius (2014)

$$6. \quad \mathrm{OCR} = \left(\frac{K_1}{K_0}\right)^{1/\beta}$$

where K_0 is the coefficient of earth stress at rest for normally consolidated sand, K_1 is the coefficient of earth stress at rest for overconsolidated (compacted) sand and β is an empirically determined exponent.

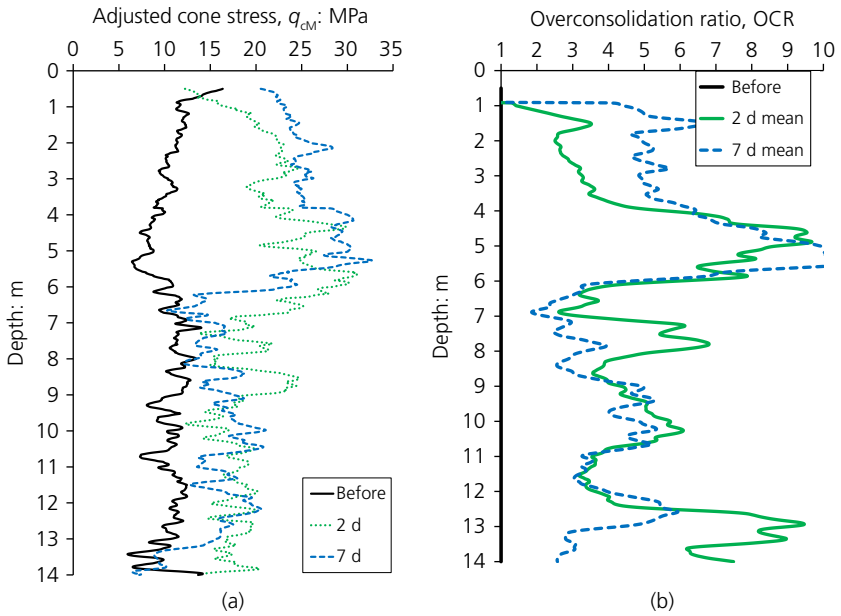

Figure 8. Evaluation of cone stress after compaction: (a) adjusted cone stress, corresponding to mean effective stress of 100 kPa; (b) OCR determined from increase in sleeve friction, assuming $\beta = 0{\cdot}45$

As a conservative assumption, $\beta = 0{\cdot}45$ can be chosen, from which the OCR can be calculated according to Equation 6. Figure 8(b) shows the variation of OCR with depth, 2 d and 7 d after compaction. The OCR values have been averaged over depth intervals of ±100 mm. The OCR increased from the uncompacted sand (OCR = 1) to an average value of OCR > 2. The increase in OCR is the most pronounced at depths of between 4 and 6 m (OCR > 6). The variation of q_{cM} and OCR with depth, shown in Figure 8, reflects heterogeneity. When calculating settlement in a compacted fill, it is important to take into account the preconsolidation effect (Massarsch and Fellenius, 2014).

5. Settlement calculation

The tangent modulus method is a powerful tool for calculating settlement in a wide variety of soils (CGS, 1992; Fellenius, 2017). The determination of settlement in sand fill prior to and after compaction has been described by Massarsch and Fellenius (2014). The most important aspect is the selection of realistic input parameters: modulus number and preconsolidation stress. The modulus number, m, can be correlated to the stress-adjusted cone stress, q_{cM}, as expressed by

$$7. \quad m = a\left(\frac{q_{cM}}{\sigma_r}\right)^{0{\cdot}5}$$

where a is an empirical modulus modifier, which depends on soil type, and σ_r is the reference stress = 100 kPa.

The modulus modifier, a, reflects the soil type and varies within a relatively narrow range for each soil category (Massarsch and Fellenius, 2014). Applying $a = 20$ as a representative modifier for the subject case, the distributions of the pre- and post-modulus numbers are as shown in Figure 9. The modulus number prior to compaction was ~250, but increased after compaction to between 500 (1–6 m depth) and 350 (below 6 m). In addition, the preconsolidation stress can be estimated from Figure 8(b). The OCR value in the uncompacted fill can be assumed to 1. After compaction, the OCR is between 2 and 5 or higher. It is important to recognise the significant effect of OCR (preconsolidation effect) on settlement calculation. The OCR is equally important when assessing the liquefaction potential of water-saturated sand.

5.1 Soil classification

Soil type can be evaluated according to soil behaviour type (SBT) charts where the measured cone stress is plotted in a semi-logarithmic diagram against the friction ratio. Figure 10 shows the same test records in a linear diagram of adjusted cone stress, q_{cM}, against sleeve friction, f_s. Also indicated on the scale on the right-hand side of the diagram is an approximate value of the density index, I_D (the older reference is relative density, D_R). For the evaluation of compaction projects, this manner of plotting the data adds significant information as it clearly shows the increase in sleeve friction and infers the increase in horizontal stress.

6. Conclusions

Settlement is often the critical parameter for vibratory compaction of sand fill. Therefore, it is essential to use transparent

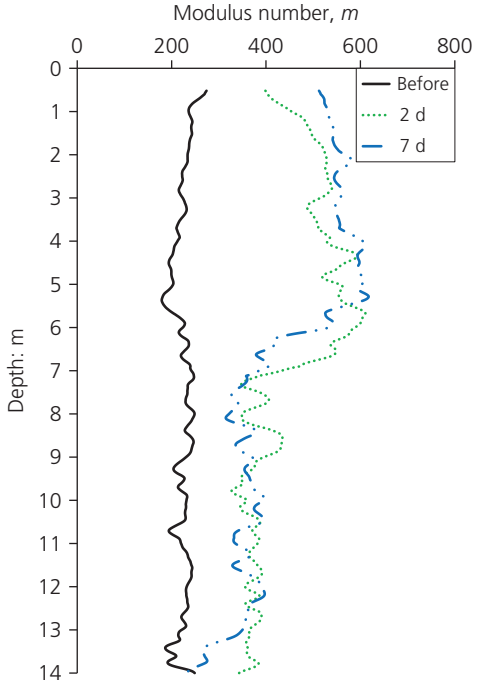

Figure 9. Variation of modulus number with depth prior to and 2 d and 7 d after compaction

methods to determine settlement prior to compaction in order to establish whether – or to what degree – compaction is required. Adjustment of cone stress with respect to the mean effective stress is an important step in the interpretation of CPT data as it represents a depth-independent parameter of soil stiffness.

A simple concept to characterise sand fill prior to – and after – compaction has been described, presenting CPT data as stress-adjusted cone stress against sleeve friction in a linear chart. This method of soil characterisation has significant advantages for compaction evaluation as compared with the more general SBT characterisation charts.

The tangent modulus method can be used for settlement analyses in all soil types, as it takes into account the stress-dependent variation of the soil modulus. The case is simplified when the tangent modulus method is applied to granular soils (silt, sand and gravel). The most important parameter for settlement analysis is the modulus number. One reason for the limited application of the tangent modulus method in compaction projects has been the uncertainty of choosing appropriate values of the modulus number prior to and after compaction. The method of estimating the modulus number based on stress-adjusted cone stress eliminates this limitation.

A case history of a 14 m thick sand fill improved by the resonance compaction method was presented. In this method, a purpose-built compaction probe with large openings is vibrated into uncompacted fill at high frequency (30 Hz). During the following compaction process, the vibration frequency is gradually lowered to the resonance frequency of the vibrator–probe–soil system. The resonance frequency was, in the actual case, about 14 Hz – that is, much lower than the conventional operating frequency of a vibrator. The total duration of compaction was 14 min, with an effective compaction time of 5 min. Due to the resonance effects, ground vibrations and thus compaction were significantly enhanced, resulting in a reduced duration of compaction and an increased compaction effect.

Extensive compaction trials were carried out. The average compression of the 14 m thick sand fill was about 4·4% and the average settlement of the area was about 0·64 m.

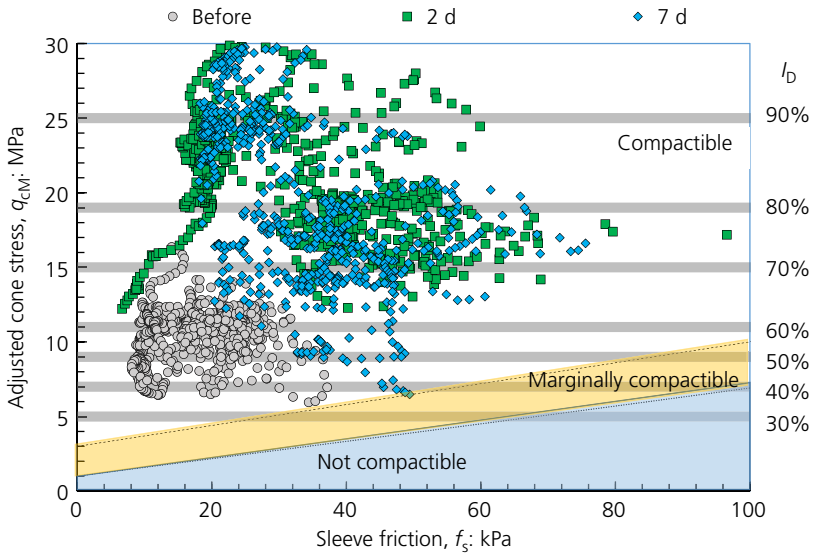

Figure 10. Soil classification based on linear relationship between sleeve friction and adjusted cone stress

To investigate the increase in cone stress and sleeve friction, CPTs were carried out prior to and 2 d and 7 d after compaction. The cone stress and sleeve friction increased significantly after compaction, on average by about a factor of two or higher. It is interesting to note that the increase in sleeve friction was more pronounced than the increase in cone stress. No clear indication could be found that cone stress or sleeve friction increased with time after the compaction work was completed.

An important aspect of vibratory compaction of sand is the permanent preconsolidation effect, which is reflected by the increase in sleeve friction. It can be assumed that sand fill prior to compaction is normally consolidated. This preconsolidation effect can be estimated from the increase in sleeve friction prior to and after compaction. From the increase in horizontal earth stress, the OCR can be estimated. This effect is often neglected, but needs to be taken into account in settlement analyses in order to obtain realistic results.

The case history presented illustrates how the soil modulus, m, and the OCR can be determined prior to and after compaction, based on CPT results. The modulus number increased from $m = 200$ prior to compaction to more than $m = 500$ after compaction. The OCR increased from 1 (normally consolidated sand) to between 2 and 5 (or higher).

REFERENCES

Balachowsky L and Kurek N (2016) Vibroflotation control of sandy soils using DMT and CPTU. *Proceedings of the 3rd International Conference on the Flat Dilatometer, DMT'15, Rome, Italy*, pp. 185–190.

Bo WM, Arulrajah A, Horpibulsuk S, Leong M and Disfani MM (2014) Densification of land reclamation sands by deep vibratory compaction. *Journal of Materials in Civil Engineering* **26(8)**: 06014016-1–06014016-6.

Brown DF (1989) *Evaluation of the Tri Star Vibro Compaction Probe*. Master's thesis, The University of British Columbia, Vancouver, BC, Canada.

CGS (Canadian Geotechnical Society) (1992) *Canadian Foundation Engineering Manual*, 3rd edn. BiTech Publishers, Richmond, BC, Canada.

Choa V, Bo MW and Chu J (2001) Soil improvement works for Changi East Reclamation Project. *Ground Improvement* **5(4)**: 141–153.

Fellenius BH (2017) *Basics of Foundation Design – A Textbook*. Pile Buck International, Inc., Vero Beach, FL, USA, electronic edition. See http://www.Fellenius.net (accessed 22/05/2017).

Gallon A and Netterman K (1996) *Time-Dependent Change of Soil Properties in Hydraulic Fill after MRC-Compaction*. Department of Soil and Rock Mechanics, Royal Institute of Technology (KTH), Stockholm, Sweden, report 96/10.

Jáky J (1948) Pressure in silos. *Proceedings of the 2nd ICSMFE, Rotterdam, the Netherlands*, vol. 1, pp. 103–107.

Jendeby L (1992) Djuppackning med Vibro-sond av typ Vibro-wing. (Deep Compaction by Vibrowing). *Proceedings of Nordic Geotechnical Meeting NGM-92, Aalborg, Denmark*, vol. 1, pp. 19–24 (in Swedish).

Krogh P and Lindgren A (1997) *Dynamic Field Measurements During Deep Compaction at Changi Airport, Singapore*. Department of Soil and Rock Mechanics, Royal Institute of Technology (KTH), Stockholm, Sweden, report 97/9.

Lee KM (2001) Influence of placement method on the cone penetration resistance of hydraulically placed sand fills. *Canadian Geotechnical Journal* **38(3)**: 592–607.

Massarsch KR (1991a) Deep vibratory compaction of land fill using soil resonance. *Proceedings of International Workshop on Technology for Hong Kong's Infrastructure Development, Infrastructure'91, Hong Kong Airport Authorities, Hong Kong*, pp. 677–697.

Massarsch KR (1991b) Deep soil compaction using vibratory probes. In *Symposium on Design, Construction, and Testing of Deep Foundation Improvement: Stone Columns and Related Techniques, Philadelphia, PA, USA* (Bachus RC (ed.)). ASTM, West Conshohocken, PA, USA, ASTM STP 1089, pp. 297–319.

Massarsch KR (1994) Design aspects of deep soil compaction. In *Proceedings of Seminar on Ground Improvement Methods*. Geotechnical Division, Hong Kong Institution of Engineers, Hong Kong, pp. 61–74.

Massarsch KR (2002) Effects of vibratory compaction. *Proceedings of TransVib 2002 – International Conference on Vibratory Pile Driving and Deep Soil Compaction, Louvain-la-Neuve, Belgium*, Keynote Lecture, pp. 33–42.

Massarsch KR and Broms BB (1983) Soil compaction by VibroWing method. *Proceedings of the 8th European Conference on Soil Mechanics and Foundation Engineering, Helsinki, Finland*, vol. 1, pp. 275–278.

Massarsch KR and Fellenius BH (2005) Deep vibratory compaction of granular soils. In *Ground Improvement – Case Histories* (Indraratna B and Chu J (eds)). Elsevier, Oxford, UK, vol. 3, chapter 19, pp. 633–658.

Massarsch KR and Fellenius BH (2014) Use of CPT for design, monitoring and performance verification of compaction projects. In *Proceedings of the 3rd International Symposium on Cone Penetration Testing, Las Vegas, Nevada* (Robertson PK and Cabal KL (eds)). Omnipress, Las Vegas, NV, USA, pp. 1187–1200.

Neely WJ and Leroy DA (1991) Densification of sand using a variable frequency vibratory probe. In *Symposium on Design, Construction, and Testing of Deep Foundation Improvement: Stone Columns and Related Techniques, Philadelphia, PA, USA* (Bachus RC (ed.)). ASTM, West Conshohocken, PA, USA, ASTM STP 1089, pp. 320–332.

Van Impe VF, De Cock F, Massarsch KR and Mengé P (1994) Recent experiences and developments of the resonant vibrocompaction technique. *Proceedings of the 13th International Conference on Soil Mechanics and Foundation Engineering, New Delhi, India*, vol. 3, pp. 1151–1156.